论 著

能谱CT成像定量参数对IA期肺腺癌高级别模式的评估价值*

宁芳卫[1] 张鹏娟[1] 袁 博[1]
张中冕[2,*]
1.郑州大学第二附属医院医学影像科
2.郑州大学第二附属医院肿瘤科
(河南 郑州 450014)

【摘要】**目的** 探讨能谱CT成像定量参数对IA期肺腺癌高级别模式(HGP)的评估价值，以期为临床制定干预治疗方案提供参考。**方法** 选取2020年1月至2024年6月IA期肺腺癌患者98例，根据手术病理检查结果分为HGP组与非HGP(non-HGP)组，术前均行能谱CT检查，比较两组能谱CT定量参数[动静脉期碘基值(IC)、标准化碘基值(NIC)、水基值(WC)、曲线斜率(K)、平均CT值]，分析各参数对HGP的单独及联合评估价值。**结果** HGP组动静脉期WC、K、平均CT值高于non-HGP组(P＜0.05)；动脉期WC、静脉期WC、动脉期K、静脉期K、平均CT值评估IA期肺腺癌HGP的AUC分别为0.798、0.759、0.731、0.749、0.784，敏感度分别为68.18%、72.73%、68.18%、63.64%、81.82%，特异度分别为88.16%、73.68%、75.00%、85.53%、73.68%；危险度分析显示，动脉期WC、静脉期WC、动脉期K、静脉期K、平均CT值高值提示IA期肺腺癌HGP的风险增加倍(P＜0.05)；动脉期WC、静脉期WC、动脉期K、静脉期K、平均CT值联合评估IA期肺腺癌HGP的AUC为0.903，敏感度为86.36%，特异度为89.47%，评估价值优于各参数单独评估价值(P＜0.05)。**结论** 能谱CT成像定量参数可用于IA期肺腺癌HGP评估中，为临床早期鉴别IA期肺腺癌HGP、针对性制定干预治疗方案提供参考依据。

【关键词】肺腺癌；高级别模式；能谱CT成像；定量参数；鉴别
【中图分类号】R563
【文献标识码】A
【基金项目】北京医卫健康公益基金会《医学科学研究基金资助项目》(YWJKJJHKJJ-B182134)
DOI:10.3969/j.issn.1672-5131.2026.04.015

The Evaluation Value of Quantitative Parameters of Spectral CT Imaging for High-grade Patterns of Stage IA Lung Adenocarcinoma*

NING Fang-wei[1], ZHANG Peng-juan[1], YUAN Bo[1], ZHANG Zhong-mian[2,*].
1.Department of Medical Imaging, Second Affiliated Hospital of Zhengzhou University, Zhengzhou 450014, Henan Province, China
2.Department of Oncology, Second Affiliated Hospital of Zhengzhou University, Zhengzhou 450014, Henan Province, China

ABSTRACT
Objective To explore the evaluation value of quantitative parameters of spectral CT imaging for high-grade pattern (HGP) of stage IA lung adenocarcinoma, with a view to providing reference for clinical intervention treatment planning. ***Methods*** A total of 98 patients with lung adenocarcinoma in the IA stage from January 2020 to June 2024 were selected and divided into the HGP group and the non-HGP group based on surgical pathology results. All patients underwent spectral CT examination before surgery. The quantitative parameters of spectral CT [arteriovenous iodine base value (IC), normalized iodine base value (NIC), water base value (WC), curve slope (K), average CT value] were compared in the two groups, and the individual and combined evaluation value of each parameter for HGP were analyzed. ***Results*** The WC, K, and average CT values in the arteriovenous phase of the HGP group were higher than those in the non-HGP group (*P*<0.05). The AUCs of WC in the arterial phase, WC in the venous phase, K in the arterial phase, K in the venous phase, and mean CT value for evaluating HGP in stage IA lung adenocarcinoma were 0.798, 0.759, 0.731, 0.749, and 0.784, respectively. The sensitivities were 68.18%, 72.73%, 68.18%, 63.64%, and 81.82%, respectively, and the specificities were 88.16%, 73.68%, 75.00%, 85.53%, and 73.68%, respectively. The risk analysis showed that the high values of WC in the arterial phase, WC in the venous phase, K in the arterial phase, K in the venous phase, and average CT value were associated with an increased risk of HGP in stage IA lung adenocarcinoma (*P*<0.05). The combined assessment of WC in the arterial phase, WC in the venous phase, K in the arterial phase, K in the venous phase, and the average CT value for the evaluation of HGP in stage IA lung adenocarcinoma had an AUC of 0.903, with a sensitivity of 86.36% and a specificity of 89.47%. The evaluation value was superior to that of each parameter evaluated individually (*P*<0.05). ***Conclusion*** The quantitative parameters of spectral CT imaging can be used in the evaluation of HGP in stage IA lung adenocarcinoma, providing a reference for early clinical identification of HGP in stage IA lung adenocarcinoma and targeted intervention treatment plans.
Keywords: Lung Adenocarcinoma; High-Grade Pattern; Spectral CT Imaging; Quantitative Parameters; Identify

肺腺癌为肺癌的主要组织学亚型，其中IA期肺腺癌大多数患者预后良好，但仍有15%左右患者存在隐匿性淋巴结转移[1]。目前临床将高级别生长方式占比≥20%的肺腺癌定义为高级别模式(HGP)肺腺癌，相较于非HGP肺腺癌具有较高复发率，且更易出现淋巴结转移，对患者生命安全造成严重威胁[2-3]。能谱CT成像为近年来新型成像技术，可为肺腺癌早期诊断提供分析工具及定量分析指标，通过形态学及功能学等参数信息，可对肺癌进行多维度判读，利用能谱曲线斜率(k)、碘浓度(IC)等参数可定量评估组织成分、反映组织血流灌注信息等[4-6]。但目前临床关于能谱CT成像对肺腺癌HGP评估价值的相关研究较为少见，基于此，本研究试分析能谱CT成像定量参数对IA期肺腺癌HGP的评估价值，以期为临床早期鉴别、制定干预治疗方案提供参考。

1 资料与方法

1.1 一般资料 经我院伦理委员会审核批准，选取2020年1月至2024年6月IA期肺腺癌患者98例，其中男55例，女43例，年龄(58.42±4.28)岁；体重指数(BMI)(21.92±1.46)kg/m^2。

纳入标准：(1)均经影像学检查、病理学检查确诊为肺腺癌，且临床分期为IA期；(2)病灶最大径≤3cm；(3)检查前均未接受相关治疗干预；(4)患者知晓本研究，并签订知情同意书。排除标准：(1)合并其他恶性肿瘤；(2)全身感染性疾病者；(3)严重脏器功能障碍者；(4)合并能谱CT检查绝对禁忌症者；(5)既往有恶性肿瘤病史者；(6)合并精神疾病或检查依从性较差者。

1.2 方法 能谱CT检查：均采用美国GE 256层Revolution CT扫描仪进行胸部检查，检查前去除可能影响X线穿透性物品。患者取仰卧位，检查过程中保持身体不移动，患者深吸气后屏气扫描，扫描范围为肺尖至肺底。先行能谱CT平扫，能谱成像平扫参数：层厚5 mm，层间距5 mm，螺距1.375 : 1，探测器宽度40 mm，矩阵512×512，噪声指数12，旋转时间0.5 s。增强扫描条件及参数同平扫模式，经肘静脉注射非离子型对比剂碘海醇(350 mgI/mL)，剂量1.0 ml/kg，注射速率2.5 mL/s，对比剂注射完成后注射30 ml

【第一作者】宁芳卫，女，主治医师，主要研究方向：CT或MRI。E-mail：ningfang14789@126.com
【通讯作者】张中冕，男，主任医师，主要研究方向：肺癌靶向治疗及免疫治疗。E-mail：290461694@qq.com

生理盐水，能谱CT动脉期及静脉期扫描分别于注射后30 s及60 s进行，扫描结束后将所有图像数据上传至AW4.7后处理工作站进行分析处理。

图像处理及数据测量：均由同两名具有10年以上工作经验的胸部CT诊断医师分析图像及数据测量，选择Stnd重建方式，重建为层厚0.625mm、层间距0.625mm的薄层图像，采用GSI Viewer软件进行数据分析，选取GSI胸部平扫序列，设置为肺窗，在70 keV单能量横断面图像上观察分析形态学征象。分别选取GSI胸部动脉期、静脉期序列，设置为70 keV单能量横断面肺窗，选取结节最大层面放置感兴趣区(ROI)绘制能谱曲线图，计算K，分别在结节最大层面及其相邻上下层面放置ROI，测量IC和水基值(WC)，并计算标准化碘基值(NIC)，NIC=ICR(病灶碘浓度)/RCA(主动脉弓层面主动脉碘浓度)。

1.3 观察指标 (1)比较两组基本资料。(2)比较两组能谱CT定量参数(K、IC、NIC、WC)。(3)分析能谱CT定量参数对IA期肺腺癌HGP的评估价值。(4)分析能谱CT定量参数与IA期肺腺癌HGP的危险度。

1.4 统计学方法 采用SPSS 28.0软件处理分析相关数据，符合正态分布的计量资料用($\bar{x}\pm s$)表示，两组间比较采用独立样本t检验，计数资料用n(%)表示，两组间比较行χ^2检验，评估价值分析采用受试者工作特征(ROC)曲线，不同预测方案间AUC比较采用DeLong检验，联合预测实施Logistic二元回归拟合，获得返回预测概率logit(p)，将其作为独立检验变量进行ROC分析，危险度分析不同水平能谱CT定量参数患者IA期肺腺癌HGP风险，默认双侧检验，$P<0.05$表示差异有统计学意义。

2 结　果

2.1 基本资料 两组性别、年龄、BMI、吸烟史、饮酒史、肿瘤家族史等基本资料比较，差异无统计学意义(P＞0.05)，见表1。

2.2 两组能谱CT定量参数 两组动静脉期IC、NIC比较，差异无统计学意义(P＞0.05)；HGP组动静脉期WC、K、平均CT值高于non-HGP组(P＜0.05)，见表2。

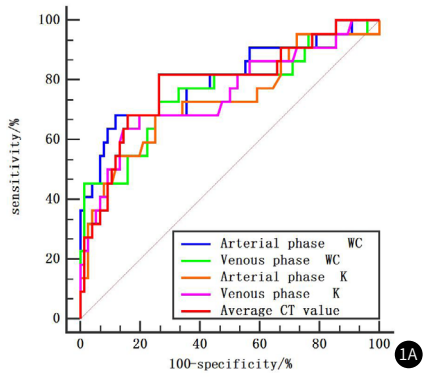
2.3 能谱CT定量参数对IA期肺腺癌HGP的评估价值 以两组能谱CT定量参数作为源数据，HGP组作为阳性数据样本，non-HGP组作为阴性数据样本，绘制ROC曲线，结果显示，动脉期WC、静脉期WC、动脉期K、静脉期K、平均CT值评估IA期肺腺癌HGP的AUC分别为0.798、0.759、0.731、0.749、0.784，最佳截断值分别为629.20 mg/cm3、572.59 mg/cm^3、3.86、3.50、-431.58 HU，敏感度分别为68.18%、72.73%、68.18%、63.64%、81.82%，特异度分别为88.16%、73.68%、75.00%、85.53%、73.68%。将动脉期WC、静脉期WC、动脉期K、静脉期K、平均CT值进行综合回归，建立Logistic诊断评估模型，再依据所得回归系数B，归一化加权计算并对应处理各样本资料，并据其进行联合应用的ROC分析，结果显示，上述各参数联合评估IA期肺腺癌HGP的AUC为0.903，敏感度为86.36%，特异度为89.47%，评估价值优于各参数单独评估价值($P<0.05$)，见图1、表3。

表1 两组基本资料[n(%)]

Data	HGP group (n=22)	non-HGP group (n=76)	t/χ^2	P
Gender			0.102	0.750
Male	13(59.09)	42(55.26)		
Female	9(40.91)	34(44.74)		
Age (years)	58.69±4.41	58.27±4.09	0.417	0.678
BMI(kg/m^2)	22.04±1.55	21.76±1.38	0.815	0.417
Smoking history			0.259	0.611
Yes	7(31.82)	20(26.32)		
No	15(68.18)	56(73.68)		
Drinking history			0.153	0.696
Yes	10(45.45)	31(40.79)		
No	12(54.55)	45(59.21)		
Family history of tumor			0.033	0.857
Yes	2(9.09)	6(7.89)		
No	20(90.91)	70(92.11)		

表2 两组能谱CT定量参数

	HGP group (n=22)	non-HGP group (n=76)	t/χ^2	P
Arterial phase				
IC(100 μg/cm^3)	23.16±5.31	24.28±6.02	0.788	0.433
NIC	0.30±0.06	0.29±0.05	0.789	0.432
WC(mg/cm^3)	682.59±125.93	535.72±108.45	5.392	＜0.001
K	4.21±0.94	3.30±0.81	4.474	＜0.001
Venous phase				
IC(100 μg/cm^3)	19.10±4.55	19.73±4.12	0.617	0.539
NIC	0.43±0.12	0.44±0.10	0.395	0.694
WC(mg/cm^3)	632.75±131.08	511.68±112.54	4.280	＜0.001
K	3.79±0.67	3.13±0.60	4.426	＜0.001
Average CT value (HU)	-383.38±72.49	-460.53±63.22	4.876	＜0.001



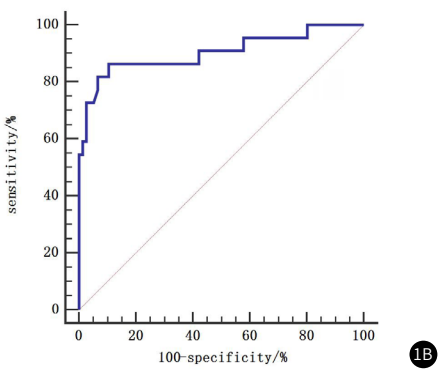


图1A～图1B 能谱CT定量参数对IA期肺腺癌HGP的评估价值

表3 AUC对比结果

Paired comparison	AUC difference	Standard error	95%CI	Z	P
Joint vs arterial phase WC	0.105	0.053	0.005~0.258	2.347	0.038
Joint vs venous phase WC	0.144	0.055	0.028~0.317	2.637	0.016
Joint vs arterial phase K	0.172	0.055	0.013~0.358	2.818	0.007
Joint vs venous phase K	0.154	0.057	0.017~0.325	2.761	0.007
Joint vs average CT value	0.119	0.054	0.004~0.274	2.508	0.021

2.4 能谱CT定量参数与IA期肺腺癌HGP的危险度分析 以ROC曲线获取的动脉期WC、静脉期WC、动脉期K、静脉期K、平均CT值最佳截断值分为低值与高值。危险度分析显示，动脉期WC、静脉期WC、动脉期K、静脉期K、平均CT值高值提示IA期肺腺癌HGP的风险增加倍(P＜0.05)，见表4。

2.5 典型病例能谱CT影像学表现 男，51岁，手术病理检查诊断为IA期肺腺癌伴有HGP，能谱CT影像学表现见图2。

表4 能谱CT定量参数与IA期肺腺癌HGP的危险度分析

Index		HGP group (n=22)	non-HGP group (n=76)	RR(95%CI)	U	P
Arterial phase WC	High value	15	9	5.758(2.927~11.326)	4.703	＜0.001
	Low value	7	67			
Venous phase WC	High value	16	20	2.764(1.754~4.356)	3.163	0.002
	Low value	6	56			
Arterial phase K	High value	15	19	2.727(1.683~4.420)	3.028	0.003
	Low value	7	57			
Venous phase K	High value	14	11	4.397(2.339~8.266)	4.021	＜0.001
	Low value	8	65			
Average CT value	High value	18	20	3.109(2.033~4.754)	3.682	＜0.001
	Low value	4	56			

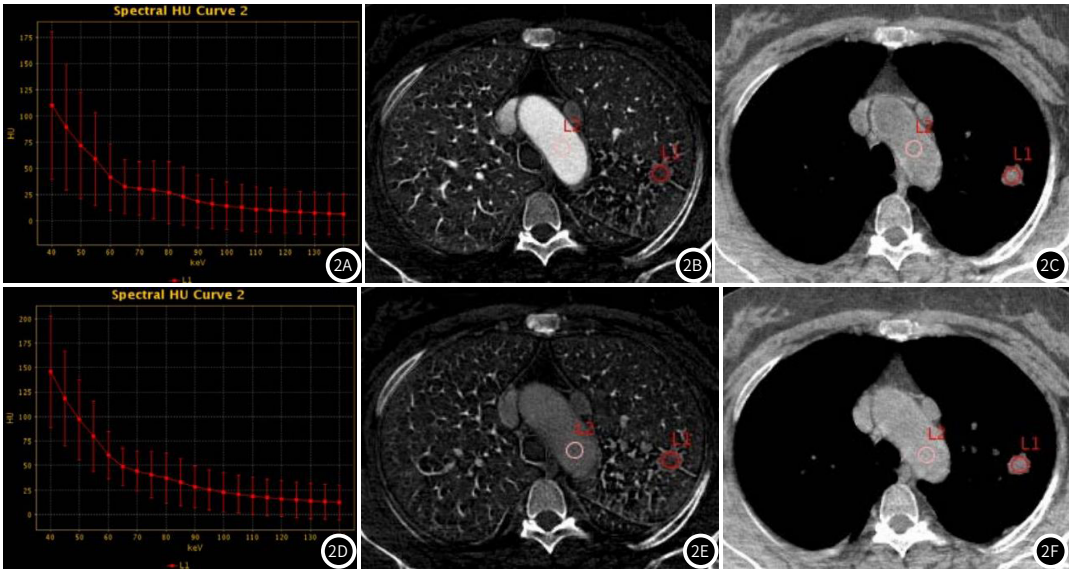


图2A 能谱曲线； **图2B** 碘基伪彩图。**图2C** 水基伪彩图； **图2D** 能谱曲线图； **图2E** 碘基伪彩图； **图2F** 水基伪彩图。

3 讨 论

肺癌具有较高发病率、病死率，其中肺腺癌为肺癌主要组织学类型，有研究表明淋巴结转移在临床分期IA期肺腺癌中较为常见，且肺腺癌组织学模式为影响早期肺癌淋巴结转移的主要因素，而肺腺癌HGP相较于非HGP更易发生淋巴结转移，从而影响患者预后恢复[7-9]。因此，早期明确IA期肺腺癌患者是否为HGP至关重要。

影像学检查目前已广泛应用于肿瘤早期诊断中，其中常规CT胸部检查仅可根据CT值变化判断病灶有无强化，但易受病灶内气体、液化坏死组织干扰，而能谱CT成像可客观、准确反映肿瘤与正常组织碘浓度差异，根据增强后碘浓度可量化组织对碘对比剂的摄取程度、反映病灶微循环状态，且通过能谱曲线可评估物质组成[10-12]。本研究结果显示，HGP组动静脉期WC、K、平均CT值高于non-HGP组，提示能谱CT成像参数对于期IA期肺腺癌HGP具有一定评估价值。IA期肺腺癌非HGP肿瘤细胞主要沿肺泡壁结构生长，组织相对疏松，而IA期肺腺癌HGP肿瘤细胞新陈代谢加快，代谢产物增多，且细胞增殖可导致肺泡壁结构破坏，细胞间隔增厚，肺泡腔内气体减少，导致水含量升高，因此动静脉期WC升高[13-15]。根据不同物质在不同单能量下衰减可获取不同CT值从而获得能谱曲线，通过能谱曲线可有效反映病灶内物质含量，而参数K可反映出不同物质的衰减特性，根据有效原子序数可对不同病灶物质组织进行准确区分[16-18]。因此IA期肺腺癌HGP与非HGP平均CT值及K具有明显差异。有研究表明[19-20]，通过能谱CT对肺部肿瘤定量分析，发现随病灶恶性程度增加，能谱曲线斜率K随之增加。另有学者[21]通过能谱CT碘基图影像组学特征对肺癌与肺部良性病灶进行鉴别诊断，发现两组平均CT值及K存在显著差异，且为肺癌的独立影响因素。进一步说明能谱CT成像参数对肺癌的评估价值。能谱CT定量参数中IC及NIC均可反映病灶血供及血管密度，病灶血供越好，血管密度越丰富，IC及NIC值越大[22-23]。但本研究中两组动静脉期IC、NIC比较无显著差异，原因可能在于，IA期肺腺癌HGP与非HGP在病理上虽存在一定差异，但病变内部微循环状态差别较小，且IA期肺腺癌恶性程度较低，肿瘤新生血管较少，因此通过动静脉期IC、NIC无法有效区分HGP与非HGP[24-25]。基于上述研究结果，本研究试通过ROC曲线分析各参数对IA期肺腺癌HGP的评估价值，结果显示动脉期WC、静脉期WC、动脉期K、静脉期K、平均CT值联合评估IA期肺腺癌HGP的AUC为0.903，敏感度为86.36%，特异度为89.47%，优于各参数单独评估价值，进一步经危险度分析显示，各参数高值可提示IA期肺腺癌HGP的风险增加倍。

（下转第74页）

[4]傅开元,胡敏,余强,等.颞下颌关节常规MRI检查规范及关节盘移位诊断标准的专家共识[J].中华口腔医学杂志,2020,55(9):608-612.
[5]Dong M,Sun Q,Yu Q,et al.Determining the optimal magnetic resonance imaging sequences for the efficient diagnosis of temporomandibular joint disorders[J].Quant Imaging Med Surg,2021,11(4):1343-1353.
[6]Guruprasad A,Sinha U,Kumar S,et al.Utility of three-dimensional proton density-weighted sequence MRI in knee for the assessment of anterolateral complex in anterior cruciate ligament injury[J].Br J Radiol,2024,97(1155):583-593.
[7]Wang Q,Zhao W,Xing X,et al.Feasibility of AI-assisted compressed sensing protocols in knee MR imaging:a prospective multi-reader study[J].Eur Radiol,2023,33(12):8585-8596.
[8]Zhao Q,Xu J,Yang YX,et al.AI-assisted accelerated MRI of the ankle:clinical practice assessment[J].Eur Radiol Exp,2023,7(1):62.
[9]Dourado GB,Volpato GH,de Almeida-Pedrin RR,et al.Likert scale vs visual analog scale for assessing facial pleasantness[J].Am J Orthod Dentofacial Orthop,2021,160(6):844-852.
[10]Sheng RF,Zheng LY,Jin KP,et al.Single-breath-hold T2WI liver MRI with deep learning-based reconstruction:a clinical feasibility study in comparison to conventional multi-breath-hold T2WI liver MRI[J].Magn Reson Imaging,2021,81:75-81.
[11]Li G,Hennig J,Raithel E,et al.An L1-norm phase constraint for half-Fourier compressed sensing in 3D MR imaging[J].MAGMA,2015,28(5):459-472.
[12]Dieckmeyer M,Roy AG,Senapati J,et al.Effect of MRI acquisition acceleration via compressed sensing and parallel imaging on brain volumetry[J].MAGMA,2021,34(4):487-497.
[13]Yunsong Liu,Zhifang Zhan,Jian-Feng Cai,et al.Projected iterative soft-thresholding algorithm for tight frames in compressed sensing magnetic resonance imaging[J].IEEE Trans Med Imaging,2016,35(9):2130-2140.
[14]Friedland S,Li Q,Schonfeld D.Compressive sensing of sparse tensors[J].IEEE Trans Image Process,2014,23(10):4438-47.
[15]范伟雄,张添辉,钟炜,等.MRI人工智能辅助压缩感知心脏电影序列在心功能评估中的应用价值[J].中国CT和MRI杂志,2024,22(9):79-81.
[16]Wang Q,Zhao W,Xing X,et al.Feasibility of AI-assisted compressed sensing protocols in knee MR imaging:a prospective multi-reader study[J].Eur Radiol,2023,33(12):8585-8596.
[17]Yoo H,Yoo RE,Choi SH,et al.Deep learning-based reconstruction for acceleration of lumbar spine MRI:a prospective comparison with standard MRI[J].Eur Radiol,2023,33(12):8656-8668..
[18]于雨洁,陈楚玥,李茗,等.基于人工智能重建算法对颅内3D FLAIR图像的优化[J].中国CT和MRI杂志,2024,22(7):34-36.
[19]Currie G,Hawk KE,Rohren E,et al.Machine learning and deep learning in medical imaging:intelligent imaging[J].J Med Imaging Radiat Sci,2019,50(4):477-487.
[20]Gore JC.Artificial intelligence in medical imaging[J].Magn Reson Imaging,2020,68:A1-A4.
[21]Castiglioni I,Rundo L,Codari M,et al.AI applications to medical images:From machine learning to deep learning[J].Phys Med,2021,83:9-24.
[22]Currie G.Intelligent imaging:anatomy of machine learning and deep learning[J].J Nucl Med Technol,2019,47(4):273-281.
[23]Topol EJ.High-performance medicine:the convergence of human and artificial intelligence[J].Nat Med,2019,25(1):44-56.
[24]Rompianesi G,Pegoraro F,Ceresa CD,et al.Artificial intelligence in the diagnosis and management of colorectal cancer liver metastases[J].World J Gastroenterol,2022,28(1):108-122.

(收稿日期：2023-04-25)　　(校对：韩敏求　排版：张鸿燊)

（上接第36页）

参考文献

[1]Keren S,Lapira M,McCallum E,et al.Paediatric orbital lymphoma; a case series and review of the literature[J].Eye (Lond),2023,37(5):1002-1008.
[2]Bagheri A,Ashtar P,Aletaha M,et al.A survey on orbital space-occupying lesions during a twelve-year period from a referral center in Iran[J].J Ophthalmic Vis Res,2023,18(2):202-211.
[3]Das L,Singh U,Malhotra B,et al.Thyroid eye disease with concurrent orbital lymphoma:a radiological surprise[J].Endocrinol Diabetes Metab Case Rep,2022,3(1):21-29.
[4]马刚,郭佩琦,崔煜艳,等.常规超声和超声造影鉴别诊断眼眶淋巴瘤与炎性假瘤[J].中国医学影像技术,2021,37(7):998-1001.
[5]Tunlayadechanont P,Panyaping T,Kaewkerd B.Role of quantitative spectral CT analysis for differentiation of orbital lymphoma and other orbital lymphoproliferative disease[J].Eur J Radiol,2020,12(133):1093-1097.
[6]Glarin RK,Nguyen BN,Cleary JO,et al.MR-EYE:High-resolution MRI of the human eye and orbit at ultrahigh field (7T) [J].Magn Reson Imaging Clin N Am,2021,29(1):103-116.
[7]孟海燕,杨维佳,黄慧莲,等.彩色多普勒超声、MRI动态增强对眼内或眶内占位病变诊断及监测价值[J].中国CT和MRI杂志,2022,20(9):28-29.
[8]Li X,Huang W,Holmes JH.Dynamic contrast-enhanced (DCE) MRI[J].Magn Reson Imaging Clin N Am,2024,32(1):47-61.
[9]Cameron CA,Tong JY,Juniat V,et al.Diagnostic utility of diffusion-weighted imaging and apparent diffusion coefficient for common orbital lesions:a review[J].Ophthalmic Plast Reconstr Surg,2022,38(6):515-521.
[10]罗清礼.眼眶恶性淋巴瘤的分类和治疗[J].中华眼科杂志,2005,41(10):9-11.
[11]Fang Y,Shen B,Dai Q,et al.Orbital inflammatory pseudotumor:new advances in diagnosis,pathogenesis,and treatment[J].Eur J Med Res,2023,28(1):395-400.
[12]赵沙沙,王文.眼眶淋巴瘤和炎性假瘤的临床表现及MRI特征[J].中华实用诊断与治疗杂志,2023,37(5):509-512.
[13]赵鑫,胥朵,李少海,等.眼眶肿瘤和瘤样病变MRI检查影像学征象及鉴别诊断研究[J].中国CT和MRI杂志,2022,20(8):47-49.
[14]王友红,柳勇,韩婷婷,等.基于MR对比增强T1WI纹理分析鉴别泪腺淋巴瘤与泪腺炎性假瘤[J].中国医学影像技术,2022,38(6):837-841.
[15]李海燕,王道芸,黄莉.眼眶炎性假瘤多层螺旋CT、磁共振影像学表现及诊断价值研究[J].中国CT和MRI杂志,2021,19(10):22-24.
[16]付珺,胡俊岭,刘强,等.分段读出序列对眼眶良恶性肿瘤的诊断价值[J].实用放射学杂志,2021,37(2):203-206,242.
[17]Eissa L,Abdel AAK,Helmy E.Arterial spin labeling and diffusion-weighted MR imaging:Utility in differentiating idiopathic orbital inflammatory pseudotumor from orbital lymphoma[J].Clin Imaging,2021,5(71):63-68.
[18]Yuan Y,Chu G,Gong T,et al.To explore MR imaging radiomics for the differentiation of orbital lymphoma and igG4-Related ophthalmic disease[J].Biomed Res Int,2021,2(14):6668-6670.
[19]Ang T,Juniat V,Patel S,et al.Evaluation of orbital lesions with DCE-MRI:a literature review[J].Orbit,2024,43(3):408-416.
[20]Pu J,Xu X,Wang P,et al.Quantitative evaluation of fibrosis in idiopathic orbital inflammatory pseudotumor by IVIM-DWI[J].Front Ophthalmol (Lausanne),2025,26(5):1545-1561.

(收稿日期：2025-08-15)
(校对：韩敏求　排版：张鸿燊)